VAMP8 contributes to TRIM6-mediated type-I interferon antiviral response during West Nile virus infection

Colm Atkins[a,*], Sarah van Tol[b,*], Preeti Bharaj[b], Ricardo Rajsbaum[b,c,#], Alexander N. Freiberg[a,c,d,#]

[a]Department of Pathology, University of Texas Medical Branch, Galveston, TX, USA

[b]Department of Microbiology and Immunology, University of Texas Medical Branch, Galveston, TX, USA

[c]Institute for Human Infections and Immunity, University of Texas Medical Branch, Galveston, TX, USA

[d]Center for Biodefense and Emerging Infectious Diseases, University of Texas Medical Branch, Galveston, TX, USA

Running Head: TRIM6 regulated WNV replication

#Address correspondence to:

Ricardo Rajsbaum, rirajsba@utmb.edu

Alexander N Freiberg, anfreibe@utmb.edu

* C.A and S.v.T. contributed equally to this work.

Abstract Word Count: 249

Text Word Count: 4047

Figures: 7

Tables: 1

ABSTRACT

Members of the tripartite motif (TRIM) family of E3 ubiquitin ligases regulate immune pathways including the antiviral type I interferon (IFN-I) system. Previously, we demonstrated that TRIM6 is involved in IFN-I induction and signaling. In absence of TRIM6 function, optimal IFN-I signaling is reduced, allowing increased replication of interferon-sensitive viruses. Despite numerous mechanisms to restrict vertebrate host's IFN-I response, West Nile Virus (WNV) replication is sensitive to pre-treatment with IFN-I. However, the regulators and products of the IFN-I pathway important in regulating WNV replications are incompletely defined. Consistent with WNV's sensitivity to IFN-I, we found that in TRIM6 knockout (TRIM6 KO) A549 cells WNV replication is significantly increased. Additionally, induction of *Ifnb* mRNA was delayed and the expression of several IFN-stimulated genes (ISGs) was reduced in TRIM6 KO cells. IFNβ pre-treatment was more effective in protecting against subsequent WNV infection in wt cells, indicating that TRIM6 contributes to the establishment of an IFN-induced antiviral response against WNV. Using next generation sequencing, we identified potential factors involved in this TRIM6-mediated antiviral response. One identified gene, VAMP8, is a soluble N-ethylmaleimide-sensitive factor attachment protein receptors (SNARE) in the vesicle-associated membrane protein subfamily. Knockdown of VAMP8 resulted in reduced STAT1 phosphorylation and impaired induction of several ISGs following WNV infection or IFNβ treatment. Therefore, VAMP8 is a novel gene involved in the regulation of IFN-I signaling, and its expression is dependent on TRIM6 function. Overall, these results indicate that TRIM6 contributes to the antiviral response against WNV by regulating the IFN-I system.

IMPORTANCE

WNV is a mosquito-borne flavivirus that poses threat to human health across large discontinuous areas throughout the world. Infection with WNV results in febrile illness, which can progress to severe neurological disease. Currently, there are no approved treatment options to control WNV infection. Understanding the cellular immune responses that regulate viral replication is important in diversifying the resources available to control WNV. Here we show that the elimination of TRIM6 in human cells results in an increase in WNV replication and alters the expression and function of other components of the IFN-I pathway through VAMP8. Dissecting the interactions between WNV and host defenses both informs basic molecular virology and promotes the development of host- and viral-targeted antiviral strategies.

INTRODUCTION

West Nile Virus (WNV) is an enveloped positive sense single stranded RNA virus and a member of the family *Flaviviridae* (1, 2). Mosquitoes competent for WNV (predominantly *Culex)* transmit the virus through blood feeding. Enzootic transmission cycles between birds and mosquitoes maintain the virus in the environment, but mosquitoes also incidentally infect humans and other mammals that act as dead-end hosts. In 1999, WNV was introduced to North America and has since then become an endemic pathogen, causing annual outbreaks in human populations, and is the leading cause of mosquito-borne encephalitis (3). Although primarily asymptomatic, WNV infection causes flu-like symptoms in approximately 20% of infected humans with fewer than 1% of symptomatic cases progressing to neurologic manifestations (4). The case fatality rate for symptomatic cases is approximately 10% (1). Currently, no WNV vaccines or anti-viral treatments are approved for human use (5–9).

Understanding the molecular mechanisms of WNV replication at the host cellular level, and specifically WNV-host IFN-I interactions, may allow identifying targets for antiviral development. Many groups have demonstrated that interferon-stimulated gene (ISG) products, such as ISG54 (IFIT2) (10), IFITM3 (11), and Oas1b (12), and others (Reviewed in: (13)) restrict WNV replication. Further, in mouse models of WNV infection, lack of IFN-I induction through signaling factors such as TLR3 (14, 15), IRF7 (14), RIG-I (16), IFNβ (2, 17), IFNAR (14), STAT1 (18), and IKKε (10) increases susceptibility to WNV. Mutations in IFN-I pathway genes and ISGs have also been associated with increased disease during WNV infections in humans (19, 20). Despite WNV's sensitivity to IFN-I, WNV has evolved several mechanisms to antagonize IFN-I including NS1 interference with RIG-I and MDA5 (21), NS3 helicase impairment of Oas1b activity (12), NS5 disruption of the type-I interferon receptor (IFNAR) surface expression (22), STAT1 phosphorylation (23), and subgenomic flavivirus RNA (24). Since WNV's resistance to IFN-I contributes to virulence (14, 25), defining the IFN-I

signaling pathway components required to respond to WNV infection is important in aiding the development of WNV-specific therapies.

Upon WNV infection, pathogen recognition receptors including RIG-I and MDA5 recognize viral RNA (16) and signal through their adaptor MAVS to activate downstream IKK-like kinases TBK1 and IKKε. Activation of TBK1 and IKKε promote IFN-I production through activation of transcription factors IRF3 and IRF7 (26). IFN-I is then secreted and engages the IFN-I receptor to induce IFN-I signaling. Early in the IFN-I signaling cascade, the kinases Jak1 and Tyk2 phosphorylate STAT1 (Y701) and STAT2 (Y690), which dimerize and interact with IRF9 to form the ISGF3 complex (27, 28). ISGF3 interacts with interferon-stimulated response element (ISRE) present in the promoter of ISGs. In addition, upon IFN-I stimulation, IKKε plays an essential role in phosphorylation of STAT1 on S708, which is required for induction of IKKε-dependent ISGs leading to an optimal antiviral response (29). Several IKKε-dependent ISGs, including ISG54, are involved in restricting WNV (10).

TRIM6, an E3 ubiquitin ligase in the tripartite motif (TRIM) protein family, plays a crucial role in facilitating the activation of the IKKε-dependent branch of the IFN-I signaling pathway. In concert with the ubiquitin activating (E1) and the E2 ubiquitin conjugating enzyme UbE2K, TRIM6 synthesizes unanchored K48-linked polyubiquitin chains that promote the oligomerization and autophosphorylation of IKKε (T501) (30). Following phosphorylation of T501, IKKε is activated and phosphorylates STAT1 (S708) to promote the transcription of the IKKε-dependent ISGs (30). Due to TRIM6's role in activating IKKε-dependent IFN-I signaling and the importance of IKKε-specific ISGs in restricting WNV, we hypothesized that WNV replication would be enhanced in the absence of TRIM6.

Here we show that WNV viral load is increased and that IFN-I induction and IKKε-dependent IFN-I signaling are impaired in TRIM6-knockout (TRIM6-KO) cells. Next-generation RNA sequencing (NGS) identified several ISGs expressed at lower levels in TRIM6-KO cells compared to wild-type (wt) cells, as well as several ISGs differentially expressed in TRIM6-KO cells previously described to

restrict WNV replication. We investigated the role of a TRIM6-dependent gene not previously described to regulate WNV replication or IFN-I signaling, *Vamp8*. VAMP8 is a vesicle-associated-membrane protein in the SNARE (Soluble-*N*-ethylmaleimide-sensitive factor attachment protein) family known to modulate endocytosis (31), exocytosis of secretory (32–35) and lytic (36) granules, thymus development (37), receptor exocytosis (38), and cross-presentation by antigen presenting cells (39). We found that VAMP8 did not directly affect WNV replication, but does promote optimal IFN-I signaling. Overall, we conclude that TRIM6 is important in promoting optimal IFN-I induction and signaling during WNV infection and that VAMP8 is a novel TRIM6-dependent factor involved in regulating IFN-I signaling.

RESULTS

WNV Replication is Increased in IFN-I Induction and Signaling Impaired TRIM6-KO Cells

To test our hypothesis that the absence of TRIM6 facilitates WNV replication, growth kinetics at a MoI of 0.1 were determined in wt and TRIM6-KO A549 cells, respectively. A significant increase in viral replication was detected in TRIM6-KO cells at 48 hours post infection (hpi) in comparison to wt cells (Figure 1A). To address the effect of the absence of TRIM6 on the IFN-I pathway, protein expression and phosphorylation of IFN-I pathway components in WNV infected cells were assessed (Figure 1B). No differences in the levels of TBK1 phosphorylation or total TBK1 expression were detected between wt and TRIM6-KO cells (Figure 1B). While the levels of pIKKε (S172), a TRIM6-independnet post-translational modification, were not significantly different between wt and TRIM6-KO cells, the TRIM6-dependent phosphorylation on IKKε (T501) was substantially lower in the TRIM6-KO cells (Figure 1B), consistent with our previous reports that TRIM6 is important for IKKε activation (30). In line with these findings, IRF3 phosphorylation, a marker of IFNβ induction, was also reduced in TRIM6-KO cells (Figure 1B). Although these results suggest that there is reduced IFN-I induction in

TRIM6-KO cells, STAT1 (Y701) phosphorylation (IKKε and TRIM6-independent (29, 30)) was not significantly affected, suggesting that there is enough IFN-I induced during WNV infection. To further characterize IFN-I signaling in TRIM6-KO cells, RNA expression levels for *ifnB* and selected ISGs were analyzed (Figure 1C). Indeed, *ifnb* mRNA is reduced in TRIM6-KO cells only at early time points p.i. and is later significantly increased as compared to wt cells (Figure 1C). The amount of total STAT1 protein, which is itself an IKKε-independent ISG (29), is substantially increased in TRIM6-KO relative to wt cells at the later time points (48-72 hp.i., Figure 1B), consistent with the higher levels of *ifnb* mRNA observed in TRIM6-KO cells (Figure 1C). The high levels of *ifnb* mRNA observed at 48 hpi in TRIM6-KO cells (Figure 1C) are probably due to the increased viral replication, and possible redundancy of other TRIM6/IKKε–independent pathways in IFN-I induction. Increased total STAT1 in TRIM6-KO cells is also consistent with the reported accumulation of unphosphorylated STAT1 in IKKε-KO cells (40) . However, phosphorylation on STAT1 (S708), an IKKε and TRIM6-dependent modification (29, 30), is nearly undetectable in the TRIM6-KO cells upon WNV infection (Figure 1B). Consistent with this defect in the TRIM6-IKKε branch of the IFN-I signaling pathway in TRIM6-KO cells, the TRIM6/IKKε-dependent ISGs *Isg54* and *Oas1* (29, 30), have different patterns of induction. In the case of *Isg54*, induction is significantly lower in the TRIM6-KO cells than in wt cells at 24 hpi, but this pattern is reversed at 72 hpi mirroring *Ifnb* expression (Figure 1C). In contrast, induction of *Oas1* is attenuated in TRIM6-KO cells 24-72 hpi (Figure 1C). IKKε-independent ISGs *Irf7* and *Stat1* and non-ISG *Il-6* are expressed at higher levels in TRIM6-KO cells at later time points (Figure 1C), again in correlation with *Ifnb* induction. Overall, the absence of TRIM6 augments WNV replication and impairs the IKKε-dependent branch of the IFN-I pathway, in line with our previous findings with other viruses including Influenza, Sendai and Encephalomyocarditis (30).

153 **IFN-I has reduced anti-WNV activity in TRIM6-deficient cells**

154 Next, we sought to evaluate further the impact of TRIM6 on the antiviral efficiency of IFN-I against
155 WNV. Prior to infection, wt and TRIM6-KO A549 cells were treated with 100U of recombinant human
156 IFNβ for 4 hours prior to infection with WNV (MoI 5.0) for 24 hours (Figure 2). Pre-treatment with IFNβ
157 decreased viral load in both wt and TRIM6-KO cells, however IFN-I pre-treatment was significantly
158 less effective in inhibiting WNV replication in TRIM6-KO (40 fold) as compared to wt controls (63
159 fold). As expected, this result indicates that IFN-I signaling is suboptimal in the absence of TRIM6,
160 enabling WNV to replicate to higher titers, and suggests that expression of TRIM6-dependent ISGs
161 may be involved in establishing an optimal IFN-I mediated anti-WNV response.

162

163 **VAMP8 is induced in a TRIM6-dependent manner**

164 To identify other genes affected as a consequence of TRIM6's absence, next generation sequencing
165 (NGS) of mock (Figure 3A) and WNV-infected (Figure 3B) wt and TRIM6-KO cells was performed.
166 During WNV infection, canonical ISGs were identified as being expressed at lower levels in the
167 TRIM6-KO compared to wt cells, which validates the methodology (Figure 3B). Several canonical
168 ISGs down-regulated in TRIM6-KO cells have previously been described to antagonize WNV
169 replication, including *Ifitm2* (41) and *-3* (11), or their loss of function is associated with increased WNV
170 susceptibility, including *Mx1* and *OasL* (42). We elected to investigate other genes not previously
171 described to regulate WNV replication or IFN-I pathways. A strongly downregulated gene in both
172 mock and infected cells, VAMP8, was chosen as a target for further mechanistic validation (Figure
173 3A).

174 After confirming that VAMP8 was expressed lower at the translational (Figure 3C) and transcriptional
175 (Figure 3D) levels in TRIM6-KO cells, the role of VAMP8 in regulating WNV replication was
176 interrogated. Therefore, wt A549 cells were transfected with a VAMP8-targeting siRNA pool or non-

targeting control siRNA (ntc) for 24 hours prior to WNV infection (MoI 0.1). VAMP8 knockdown (kd) had no measurable effect on WNV replication (Figure 4A). VAMP8-kd was validated by western blot, showing undetectable levels of protein, with a clear upregulation in VAMP8 protein by 24 hpi in ntc transfected cells (Figure 4B). Phosphorylation of IRF3 in VAMP8-kd cells was not significantly affected as compared to ntc-kd cells, suggesting there is no defect in IFN-I induction (Figure 4B). In contrast, phosphorylated STAT1 (Y701) was significantly lower in the VAMP8-kd cells at 48 and 72 hpi, suggesting impairment in IFN-I signaling (Figure 4B).

Subsequently, to examine whether VAMP8 is involved in regulation of the IFN-I signaling pathway, wt A549 cells were transfected with VAMP8-targeting or ntc siRNAs for 24 hours and treated with IFNβ for 12 hours. As expected, total STAT1 was induced in both VAMP8- and ntc-kd cells following IFNβ stimulation, but the level of total STAT1 in VAMP8-kd cells was slightly attenuated (Figure 5A). VAMP8's effect on STAT1 activation is more evident; however, with a strong reduction in the amount of pSTAT1 (Y701) (Figure 5A). Consistent with a potential role of VAMP8 in regulating STAT1 phosphorylation, mRNA expression levels upon IFNβ treatment of ISGs including *Stat1*, *Isg54*, and *Oas1* was significantly reduced in VAMP8-kd as compared to controls (Figure 5B). Overall, the above evidence supports that 1) VAMP8 expression is TRIM6-mediated, 2) VAMP8 does not directly affect WNV replication, and 3) VAMP8 is involved in positive regulation of IFN-I signaling upstream of STAT1 phosphorylation.

VAMP8 Knockdown Enhances WNV Replication in Cells Pre-treated with Type I IFN

Since VAMP8 modulates the IFN-I system, but does not appear to alter WNV replication, we examined whether exogenous IFN-I pre-treatment would reveal a functional defect in IFN-I signaling in VAMP8-kd cells during WNV infection. Prior to infection, wt A549 cells were treated with siRNA (VAMP8 or ntc) for 24 hours followed by a 16-hour treatment with IFNβ. Although IFNβ pre-treatment

reduced viral production in both groups, IFNβ treatment was less efficient in protecting VAMP8-kd cells against WNV replication as compared to ntc (ntc siRNA: 508 fold; VAMP8 siRNA: 79 fold) (Figure 6). As opposed to previous experiments showing no impact on WNV replication following VAMP8-kd, the combination of IFN-β pre-treatment and VAMP8 siRNA showed an 8-fold increase in the replication of WNV over cells treated with ntc siRNA and IFNβ. This result suggests that VAMP8 plays a functional role in IFN-I signaling during WNV infection.

DISCUSSION

Our study demonstrates the relevance of TRIM6 in regulating the IFN-I pathway during WNV infection and identifies VAMP8 as a factor functionally involved in IFN-I signaling. Extensive research has implicated the TRIM family of proteins in both regulation of the innate immune response and the restriction of viral replication (30, 43–48). Specifically, TRIM6 has been shown to facilitate the formation of unanchored K48-linked polyubiquitin chains that provide a scaffold for IKKε homo-oligomerization, ultimately resulting in IKKε activation and STAT1 phosphorylation at S708 (30). Phosphorylation of STAT1 at S708 is important to sustain IFN-I signaling and to express a unique subset of ISGs (29, 40). The relevance of IKKε-dependent gene expression has previously been described for WNV, and in the absence of ISG54 or IKKε mice have an increased susceptibility (10). These experiments served as a rationale for exploring the functional role of TRIM6 during WNV infection.

As expected, we observed an increase in WNV replication in TRIM6-KO cells in parallel with attenuated TRIM6-dependent activation of IKKε (T501 phosphorylation), IKKε-dependent STAT1 S708 phosphorylation, and IKKε-dependent gene expression. There was impaired *Ifnb* and *Isg54* mRNA induction in TRIM6-KO cells at 6 and 24 hpi, respectively, but higher levels of induction at 72 hpi. The transient effect of TRIM6 on the IFN-I pathway may be due to the increased amount of virus

at the peak of infection resulting in more cells producing IFN-I to compensate for TRIM6 deficiency. Although no other factor has been shown to synthesize the unanchored K48-polyubiquitin chains required for IKKε activation, we cannot exclude that other TRIM members or other E3-Ub ligases may compensate for the loss of TRIM6. Alternatively, TRIM6 may play important roles in other pathways (i.e. NF-κB), resulting in cytokine dysregulation and/or induction of IFNβ by TRIM6-independent pathways. Furthermore, since no difference in TBK1 phosphorylation is observed between wt and TRIM6-KO cells, it is possible that TBK1 activation is sufficient to compensate for reduced IKKε activation in the IFN production pathway. Further emergent WNV strains encode a functional 2-O methylase in their non-structural protein 5 that prohibits IFIT proteins, specifically murine ISG54 and human ISG58, from suppressing viral mRNA expression (49). Since WNV antagonizes components of this pathway, we cannot rule out the possibility that WNV proteins target TRIM6 to impede IKKε-dependent expression of WNV-restricting ISGs. For example, the matrix protein of Nipah virus (family *Paramyxoviridae*) works to promote the degradation of TRIM6 during viral infection to promote viral replication through impaired IKKε signaling and thus a blunted IFN-I response (44). WNV protein antagonism of TRIM6 could also preclude observing more severe differences in WNV replication between wt and TRIM6-KO cells. Alternatively, TRIM6 could play an essential role in IKKε-dependent signaling but could also be hijacked by a virus to facilitate viral replication. In a previous study, we showed that TRIM6 directly promotes the replication of ebolavirus (family *Filoviridae*) through interactions with VP35 and that VP35 antagonizes TRIM6's capacity to promote IFN-I signaling (43). Although we identified several ISGs differentially expressed in TRIM6-KO compared to wt cells following WNV infection, we also identified *Vamp8* to be significantly down-regulated under both basal conditions and WNV infection. VAMP8 has not been previously described to affect WNV replication or the IFN-I pathway. Although its role was not described, VAMP8 had been identified as an antiviral factor in an siRNA screen for Japanese encephalitis virus (JEV), another mosquito-borne

flavivirus (50). Here we showed, in contrast to that seen with JEV, VAMP8-kd does not directly affect WNV replication. The impairment of STAT1 Y701 phosphorylation during WNV in the VAMP8-kd cells lent evidence that VAMP8 could be involved in IFN-I signaling. Since WNV efficiently impairs IFN-I induction until nearly 24 hpi, VAMP8 depletion may not substantially impede of IFN-I signaling during WNV infection in a tissue culture system. Evaluation of VAMP8's role in IFN-I signaling in the absence of WNV infection revealed a striking impairment in STAT1 Y701 phosphorylation and a modest inhibition of ISG gene expression in VAMP8-depleted cells. Further, following IFNβ treatment, cells treated with VAMP8-targeting siRNA less efficiently antagonized WNV replication which provides support that VAMP8 mediates a functional step in the IFN-I signaling pathway.

At this point, VAMP8's role in regulating the IFN-I signaling pathway is unknown. VAMP8 is involved in endocytosis (31), vesicle-vesicle fusion (34), and exocytosis (32–35) in various cell types including leukocytes (36, 39), and various secretory (32, 33, 35) cells including human lung goblet cells. As a vesicular SNARE (v-SNARE), VAMP8 on the surface of a vesicle interacts with SNAREs on the target membrane surface to facilitate membrane fusion (32, 34, 36). Potential mechanisms of the IFN-I pathway, which VAMP8 may regulate, include surface expression of the IFNAR receptor or recycling of receptor components to the plasma membrane. VAMP8 has been described to regulate the surface expression of a water transport channel, aquaporin 2, in the kidney (38). Despite the reduced surface expression, the total amount of aquaporin 2 is higher in the cell, but it is retained in vesicles below the plasma membrane (38). Alternatively, VAMP8 might influence the secretion of factors or the oxidative condition of the microenvironment important to maintain IFN-I signaling. In phagocytic cells infected with *Leishmania*, VAMP8 regulates the transport of NADPH oxidase to the phagosome to facilitate optimal conditions for peptide loading into MHC class I molecules (39). Although VAMP8 would not be regulating phagocytosis in this model of WNV infection, it is possible that VAMP8 regulates NADPH oxidase localization affecting the oxidative environment of the infected cell and

consequently IFN-I signaling (51–53). TRIM6 may either directly affect VAMP8 expression or may act indirectly through a yet unidentified secondary factor. Dissecting this interaction will be important in further understanding TRIM6's regulation of the host's IFN-I pathway and uncovering VAMP8's novel role in IFN-I signaling. Our study indicates a new role for VAMP8 in the TRIM6 pathway of immune activation during viral infection (Figure 7).

Elucidating the interactions of the human immune system with viral infection is essential to understanding viral pathology, as well as identifying cellular targets for antiviral drug development. Our work has identified a novel IFN related host factor that is important in the regulation of WNV replication and in the life cycles of other viruses. This may provide a conserved target for the development of anti-viral strategies and for the elucidation of further conserved pathways in host-pathogen interaction.

ACKNOWLEDGEMENTS

Dr. Rajsbaum's lab was supported in part by the John Sealy Memorial Endowment Fund for Biomedical Research (UTMB), and NIH/NIAID grants R21 AI132479-01, R21 AI126012-01A1 and R01 AI134907-01. Dr. Freiberg's lab was supported in part by departmental funds and NIH/NIAID grants R33 AI102267.

MATERIALS & METHODS

Viruses & Cells: West Nile Virus (WNV) isolate 385-99 was obtained from the World Reference Center for Emerging Viruses & Arboviruses (UTMB, Dr. Robert Tesh). A549 and CCL-81 lines were obtained from the American Type Culture Collection. TRIM6 knockout cells were prepared as previously described (43). All lines were maintained in DMEM (Gibco), supplemented with 10% Fetal

Bovine Serum (Atlanta Biologicals). Infections were performed in DMEM supplemented with 2% Fetal Bovine Serum (FBS), and 1% Penicillin/Streptomycin (Gibco). For growth kinetics experiments, 150,000 wt or TRIM6-KO A549 cells/well were infected with 100µL of WNV multiplicity of infection (MoI) 0.1 or 5.0 for 1 hour at 37°C, 5% CO_2 then the inoculum was removed and washed 3 times with 1mL of 1X PBS. After the cells were washed, 1mL of DMEM supplemented with 2% FBS was added to each well. Supernatant (150µL) was collected at the designated time points for plaque assay. Plaque assays were performed in 12-well plates containing 200,000 CCL-81 cells/well. Viral samples were diluted log fold and applied to the monolayer. Following 1 hour in a humidified 37°C, 5% CO_2 incubator, semisolid overlay containing MEM, 2% Fetal Bovine Serum, 1% Penicillin/Streptomycin and 0.8% Tragacanth (Sigma Aldrich) was applied. Overlay was removed after 72 hours, and monolayers were fixed and stained with 10% Neutral Buffered Formalin (Thermo Fisher Scientific) and Crystal Violet (Sigma Aldrich). Plaques were enumerated by counting and graphed. All manipulations of infectious West Nile Virus were performed in Biological Safely Level 3 facilities at UTMB.

IFNβ Treatment: Cells were treated with either 100U (wt *vs* TRIM6 KO) or 500U (VAMP8) of recombinant human IFNβ-1a (PBL Assay Science) for either 4 hours or 12 hours prior to WNV infection.

RNA Isolation and qRT-PCR: At the indicated timepoint per experiment, media was removed from the cell monolayer, and 1mL Trizol Reagent (Thermo Fisher Scientific) was added. RNA was isolated using Zymo Direct-zol RNA Miniprep Kits as per manufacturer instruction with in-column DNase treatment. Isolated RNA was then reverse transcribed using the high capacity cDNA reverse transcription kit (Applied Biosystems). The cDNA was then diluted 1:3 in nuclease-free water

(Corning). Relative gene expression (primers listed in Supplementary Table 1) was determined using the iTaq™ Universal SYBR green (Bio-Rad) with the CFX384 instrument (Bio-Rad). The relative mRNA expression levels were analyzed using the CFX Manager software (Bio-Rad). The change in threshold cycle (ΔCT) was calculated with 18S gene served as the reference mRNA for normalization.

RNA Sequencing & Analysis: A549 (wt and TRIM6KO) cells were infected at a high MoI (5.0) and RNA isolated 24 hours post infection. RNA quality was assessed by visualization of 18S and 28S RNA bands using an Agilent BioAnalyzer 2100 (Agilent Technologies, CA); the electropherograms were used to calculate the 28S/18S ratio and the RNA Integrity Number. Poly-A+ RNA was enriched from total RNA (1 µg) using oligo dT-attached magnetic beads. First and second strand synthesis, adapter ligation and amplification of the library were performed using the Illumina TruSeq RNA Sample Preparation kit as recommended by the manufacturer (Illumina, Inc). Library quality was evaluated using an Agilent DNA-1000 chip on an Agilent 2100 Bioanalyzer. Quantification of library DNA templates was performed using qPCR and a known-size reference standard. Cluster formation of the library DNA templates was performed using the TruSeq PE Cluster Kit v3 (Illumina) and the Illumina cBot workstation using conditions recommended by the manufacturer. Paired end 50 base sequencing by synthesis was performed using TruSeq SBS kit v3 (Illumina) on an Illumina HiSeq 1500 using protocols defined by the manufacturer.

RNA-Seq Analysis: The alignment of NGS sequence reads was performed using the Spliced Transcript Alignment to a Reference (STAR) program, version 2.5.1b, using default parameters (54). We used the human hg38 assembly as a reference with the UCSC gene annotation file; both downloaded from the Illumina iGenomes website. The –quantMode GeneCounts option of STAR

provided read counts per gene, which were input into the DESeq2 (version 1.12.1) (55) differential expression analysis program to determine expression levels and differentially expressed genes.

siRNA Transfection: Transient knockdown of endogenous VAMP8 in wt A549 was done in 12-well plates. Briefly, 20 pmol of Smartpool ON-TARGETplus Non-targeting (D-001810-10-05) or ON-TARGETplus VAMP8 (L-013503-00-0005) siRNA (Dharmacon) were transfected with Lipofectamine RNAiMAX (Invitrogen) following the manufacturer's instructions. Cells were transfected with siRNA 24 hours prior to infection or IFNβ treatment. The efficiency of VAMP8 knockdown was monitored by qRT-PCR or western blot.

Western Blotting: Infected or IFNβ-treated cells were lysed in 2X Laemmli buffer with β-ME and boiled at 100^{o}C for 10 minutes prior to removal from BSL-3. For immunoblotting, proteins were resolved using SDS-polyacrylamide gel electrophoresis (4-15% SDS-PAGE) and transferred onto methanol-activated polyvinylidene difluoride (PVDF) membrane (Bio-Rad). The following primary antibodies were used: anti-pIRF3 (S396) (1:1000) (Cell Signaling), anti-total IRF3 (1:1000) (Immuno-Biological), anti-TRIM6 N-terminus (1:1000) (Sigma), anti-actin (1:2000) (Abcam), anti-pSTAT1 (Y701) (1:1000) (Cell Signaling), anti-pSTAT1 (S708) (1:2000), anti-total STAT1 (1:1000) (BD Biosciences), anti-VAMP8 (Cell Signaling) (1:500), anti-IKKε (T501) (1:1000) (Novus Biologicals), anti-IKKε (S172) (1:1000), anti-total IKKε (1:1000) (Abcam), anti-pTBK1 (S172) (1:1000) (Epitomics), anti-total TBK1 (1:1000) (Novus Biologicals). Immunoblots were developed with the following secondary antibodies: ECL anti-rabbit IgG horseradish peroxidase conjugated whole antibody from donkey (1:10,000), and ECL anti-mouse IgG horseradish peroxidase conjugated whole antibody from sheep (1:10,000) (GE Healthcare; Buckinghamshire, England). The proteins were visualized with either Pierce™ or SuperSignal® West Femto Luminol chemiluminescence substrates (Thermo Scientific).

Statistical Analysis: All analyses were performed in Graphpad Prism. All experiments were performed in triplicate. Statistical tests and measures of statistical significance are specified in the relevant figure legends. Repeated measures two-way ANOVA with Bonferroni's post-test was applied for kinetics two factor comparisons (kinetics experiments), one-way ANOVA with Tukey's post-test was used for comparing three more groups, and a student's t-test for comparing two groups.

REFERENCES

1. Gubler D, Kuno G, Alter L. 2007. Flaviviruses, p. 1153–1252. *In* Fields Virology, 5th ed. Lippincott, Williams & Wilkins, Philadelphia, PA, USA.

2. Lindenbach B, Thiel H-J, Rice C. 2007. Flaviviridae: The Viruses and Their Replication, p. 1101–1152. *In* Fields Virology, 5th ed. Lippincott, Williams & Wilkins, Philadelphia, PA, USA.

3. West Nile Virus and Other Arboviral Diseases — United States, 2013.

4. Sejvar JJ. 2014. Clinical Manifestations and Outcomes of West Nile Virus Infection. Viruses 6:606–623.

5. Dayan GH, Pugachev K, Bevilacqua J, Lang J, Monath TP. 2013. Preclinical and Clinical Development of a YFV 17 D-Based Chimeric Vaccine against West Nile Virus. Viruses 5:3048–3070.

6. Dayan GH, Bevilacqua J, Coleman D, Buldo A, Risi G. 2012. Phase II, dose ranging study of the safety and immunogenicity of single dose West Nile vaccine in healthy adults ≥50 years of age. Vaccine 30:6656–6664.

7. Tesh RB, Arroyo J, Travassos da Rosa APA, Guzman H, Xiao S-Y, Monath TP. 2002. Efficacy of Killed Virus Vaccine, Live Attenuated Chimeric Virus Vaccine, and Passive Immunization for Prevention of West Nile virus Encephalitis in Hamster Model. Emerg Infect Dis 8:1392–1397.

8. Blázquez AB, Vázquez-Calvo Á, Martín-Acebes MA, Saiz J-C. 2018. Pharmacological Inhibition of Protein Kinase C Reduces West Nile Virus Replication. Viruses 10.

9. Morrey JD, Taro BS, Siddharthan V, Wang H, Smee DF, Christensen AJ, Furuta Y. 2008. Efficacy of orally administered T-705 pyrazine analog on lethal West Nile virus infection in rodents. Antiviral Research 80:377–379.

10. Perwitasari O, Cho H, Diamond MS, Gale M. 2011. Inhibitor of κB Kinase ϵ (IKKϵ), STAT1, and IFIT2 Proteins Define Novel Innate Immune Effector Pathway against West Nile Virus Infection. J Biol Chem 286:44412–44423.

11. Gorman MJ, Poddar S, Farzan M, Diamond MS. 2016. The Interferon-Stimulated Gene Ifitm3 Restricts West Nile Virus Infection and Pathogenesis. J Virol 90:8212–8225.

12. Mertens E, Kajaste-Rudnitski A, Torres S, Funk A, Frenkiel M-P, Iteman I, Khromykh AA, Desprès P. 2010. Viral determinants in the NS3 helicase and 2K peptide that promote West Nile virus resistance to antiviral action of 2′,5′-oligoadenylate synthetase 1b. Virology 399:176–185.

13. Lazear HM, Diamond MS. 2015. New Insights into Innate Immune Restriction of West Nile Virus Infection. Curr Opin Virol 11:1–6.

14. Daffis S, Lazear HM, Liu WJ, Audsley M, Engle M, Khromykh AA, Diamond MS. 2011. The Naturally Attenuated Kunjin Strain of West Nile Virus Shows Enhanced Sensitivity to the Host Type I Interferon Response. J Virol 85:5664–5668.

15. Daffis S, Samuel MA, Suthar MS, Gale M, Diamond MS. 2008. Toll-Like Receptor 3 Has a Protective Role against West Nile Virus Infection. J Virol 82:10349–10358.

16. Errett JS, Suthar MS, McMillan A, Diamond MS, Gale M. 2013. The Essential, Nonredundant Roles of RIG-I and MDA5 in Detecting and Controlling West Nile Virus Infection. J Virol 87:11416–11425.

17. Lazear HM, Pinto AK, Vogt MR, Gale M, Diamond MS. 2011. Beta Interferon Controls West Nile Virus Infection and Pathogenesis in Mice. J Virol 85:7186–7194.

18. Larena M, Lobigs M. 2017. Partial dysfunction of STAT1 profoundly reduces host resistance to flaviviral infection. Virology 506:1–6.

19. Suthar MS, Diamond MS, Jr MG. 2013. West Nile virus infection and immunity. Nature Reviews Microbiology 11:115–128.

20. Petersen LR, Brault AC, Nasci RS. 2013. West Nile Virus: Review of the Literature. JAMA 310:308–315.

21. Zhang H-L, Ye H-Q, Liu S-Q, Deng C-L, Li X-D, Shi P-Y, Zhang B. 2017. West Nile Virus NS1 Antagonizes Interferon Beta Production by Targeting RIG-I and MDA5. J Virol 91.

22. Lubick KJ, Robertson SJ, McNally KL, Freedman BA, Rasmussen AL, Taylor RT, Walts AD, Tsuruda S, Sakai M, Ishizuka M, Boer EF, Foster EC, Chiramel AI, Addison CB, Green R, Kastner DL, Katze MG, Holland SM, Forlino A, Freeman AF, Boehm M, Yoshii K, Best SM. 2015. Flavivirus Antagonism of Type I Interferon Signaling Reveals Prolidase as a Regulator of IFNAR1 Surface Expression. Cell Host & Microbe 18:61–74.

23. Laurent-Rolle M, Boer EF, Lubick KJ, Wolfinbarger JB, Carmody AB, Rockx B, Liu W, Ashour J, Shupert WL, Holbrook MR, Barrett AD, Mason PW, Bloom ME, García-Sastre A, Khromykh AA, Best SM. 2010.

428 The NS5 Protein of the Virulent West Nile Virus NY99 Strain Is a Potent Antagonist of Type I Interferon-
429 Mediated JAK-STAT Signaling. J Virol 84:3503–3515.

430 24. Schuessler A, Funk A, Lazear HM, Cooper DA, Torres S, Daffis S, Jha BK, Kumagai Y, Takeuchi O,
431 Hertzog P, Silverman R, Akira S, Barton DJ, Diamond MS, Khromykh AA. 2012. West Nile Virus
432 Noncoding Subgenomic RNA Contributes to Viral Evasion of the Type I Interferon-Mediated Antiviral
433 Response. J Virol 86:5708–5718.

434 25. Keller BC, Fredericksen BL, Samuel MA, Mock RE, Mason PW, Diamond MS, Gale M. 2006. Resistance
435 to Alpha/Beta Interferon Is a Determinant of West Nile Virus Replication Fitness and Virulence. J Virol
436 80:9424–9434.

437 26. Sharma S, tenOever BR, Grandvaux N, Zhou G-P, Lin R, Hiscott J. 2003. Triggering the Interferon
438 Antiviral Response Through an IKK-Related Pathway. Science 300:1148–1151.

439 27. Paul A, Tang TH, Ng SK. 2018. Interferon Regulatory Factor 9 Structure and Regulation. Front Immunol 9.

440 28. Fu XY, Kessler DS, Veals SA, Levy DE, Darnell JE. 1990. ISGF3, the transcriptional activator induced by
441 interferon alpha, consists of multiple interacting polypeptide chains. Proc Natl Acad Sci U S A 87:8555–
442 8559.

443 29. tenOever BR, Ng S-L, Chua MA, McWhirter SM, García-Sastre A, Maniatis T. 2007. Multiple Functions of
444 the IKK-Related Kinase IKKε in Interferon-Mediated Antiviral Immunity. Science 315:1274–1278.

445 30. Rajsbaum R, Versteeg GA, Schmid S, Maestre AM, Belicha-Villanueva A, Martínez-Romero C, Patel JR,
446 Morrison J, Pisanelli G, Miorin L, Laurent-Rolle M, Moulton HM, Stein DA, Fernandez-Sesma A,
447 tenOever BR, García-Sastre A. 2014. Unanchored K48-Linked Polyubiquitin Synthesized by the E3-

Ubiquitin Ligase TRIM6 Stimulates the Interferon-IKKε Kinase-Mediated Antiviral Response. Immunity 40:880–895.

31. Antonin W, Holroyd C, Tikkanen R, Höning S, Jahn R, Pfeffer SR. 2000. The R-SNARE Endobrevin/VAMP-8 Mediates Homotypic Fusion of Early Endosomes and Late Endosomes. MBoC 11:3289–3298.

32. Wang C-C, Ng CP, Lu L, Atlashkin V, Zhang W, Seet L-F, Hong W. 2004. A Role of VAMP8/Endobrevin in Regulated Exocytosis of Pancreatic Acinar Cells. Developmental Cell 7:359–371.

33. Wang C-C, Shi H, Guo K, Ng CP, Li J, Qi Gan B, Chien Liew H, Leinonen J, Rajaniemi H, Hong Zhou Z, Zeng Q, Hong W, Malhotra V. 2007. VAMP8/Endobrevin as a General Vesicular SNARE for Regulated Exocytosis of the Exocrine System. MBoC 18:1056–1063.

34. Behrendorff N, Dolai S, Hong W, Gaisano HY, Thorn P. 2011. Vesicle-associated Membrane Protein 8 (VAMP8) Is a SNARE (Soluble N-Ethylmaleimide-sensitive Factor Attachment Protein Receptor) Selectively Required for Sequential Granule-to-granule Fusion. J Biol Chem 286:29627–29634.

35. Jones LC, Moussa L, Fulcher ML, Zhu Y, Hudson EJ, O'Neal WK, Randell SH, Lazarowski ER, Boucher RC, Kreda SM. 2012. VAMP8 is a vesicle SNARE that regulates mucin secretion in airway goblet cells. J Physiol 590:545–562.

36. Loo LS, Hwang L-A, Ong YM, Tay HS, Wang C-C, Hong W. A role for endobrevin/VAMP8 in CTL lytic granule exocytosis. European Journal of Immunology 39:3520–3528.

37. Kanwar N, Fayyazi A, Backofen B, Nitsche M, Dressel R, Fischer von Mollard G. 2008. Thymic alterations in mice deficient for the SNARE protein VAMP8/endobrevin. Cell Tissue Res 334:227–242.

468 38. Wang C-C, Ng CP, Shi H, Liew HC, Guo K, Zeng Q, Hong W. 2010. A Role for VAMP8/Endobrevin in
469 Surface Deployment of the Water Channel Aquaporin 2. Mol Cell Biol 30:333–343.

470 39. Matheoud D, Moradin N, Bellemare-Pelletier A, Shio MT, Hong WJ, Olivier M, Gagnon É, Desjardins M,
471 Descoteaux A. 2013. Leishmania Evades Host Immunity by Inhibiting Antigen Cross-Presentation through
472 Direct Cleavage of the SNARE VAMP8. Cell Host & Microbe 14:15–25.

473 40. Ng S-L, Friedman BA, Schmid S, Gertz J, Myers RM, tenOever BR, Maniatis T. 2011. IκB kinase ε (IKKε)
474 regulates the balance between type I and type II interferon responses. PNAS 108:21170–21175.

475 41. Jiang D, Weidner JM, Qing M, Pan X-B, Guo H, Xu C, Zhang X, Birk A, Chang J, Shi P-Y, Block TM,
476 Guo J-T. 2010. Identification of Five Interferon-Induced Cellular Proteins That Inhibit West Nile Virus and
477 Dengue Virus Infections. J Virol 84:8332–8341.

478 42. Danial-Farran N, Eghbaria S, Schwartz N, Kra-Oz Z, Bisharat N. 2015. Genetic variants associated with
479 susceptibility of Ashkenazi Jews to West Nile virus infection. Epidemiology & Infection 143:857–863.

480 43. Bharaj P, Atkins C, Luthra P, Giraldo MI, Dawes BE, Miorin L, Johnson JR, Krogan NJ, Basler CF,
481 Freiberg AN, Rajsbaum R. 2017. The Host E3-Ubiquitin Ligase TRIM6 Ubiquitinates the Ebola Virus
482 VP35 Protein and Promotes Virus Replication. J Virol 91:e00833-17.

483 44. Bharaj P, Wang YE, Dawes BE, Yun TE, Park A, Yen B, Basler CF, Freiberg AN, Lee B, Rajsbaum R.
484 2016. The Matrix Protein of Nipah Virus Targets the E3-Ubiquitin Ligase TRIM6 to Inhibit the IKKε
485 Kinase-Mediated Type-I IFN Antiviral Response. PLOS Pathogens 12:e1005880.

486 45. Uchil PD, Hinz A, Siegel S, Coenen-Stass A, Pertel T, Luban J, Mothes W. 2013. TRIM Protein-Mediated
487 Regulation of Inflammatory and Innate Immune Signaling and Its Association with Antiretroviral Activity.
488 J Virol 87:257–272.

46. van Tol S, Hage A, Giraldo MI, Bharaj P, Rajsbaum R. 2017. The TRIMendous Role of TRIMs in Virus–Host Interactions. Vaccines 5:23.

47. Versteeg GA, Benke S, García-Sastre A, Rajsbaum R. 2014. InTRIMsic immunity: Positive and negative regulation of immune signaling by tripartite motif proteins. Cytokine Growth Factor Rev 25:563–576.

48. Versteeg GA, Rajsbaum R, Sánchez-Aparicio MT, Maestre AM, Valdiviezo J, Shi M, Inn K-S, Fernandez-Sesma A, Jung J, García-Sastre A. 2013. The E3-ligase TRIM family of proteins regulates signaling pathways triggered by innate immune pattern-recognition receptors. Immunity 38:384–398.

49. Daffis S, Szretter KJ, Schriewer J, Li J, Youn S, Errett J, Lin T-Y, Schneller S, Zust R, Dong H, Thiel V, Sen GC, Fensterl V, Klimstra WB, Pierson TC, Buller RM, Jr MG, Shi P-Y, Diamond MS. 2010. 2′-O methylation of the viral mRNA cap evades host restriction by IFIT family members. Nature 468:452–456.

50. Zhang L-K, Chai F, Li H-Y, Xiao G, Guo L. 2013. Identification of Host Proteins Involved in Japanese Encephalitis Virus Infection by Quantitative Proteomics Analysis. J Proteome Res 12:2666–2678.

51. Olofsson P, Nerstedt A, Hultqvist M, Nilsson EC, Andersson S, Bergelin A, Holmdahl R. 2007. Arthritis suppression by NADPH activation operates through an interferon-β pathway. BMC Biol 5:19.

52. Quiroga AD, Alvarez M de L, Parody JP, Ronco MT, Francés DE, Pisani GB, Carnovale CE, Carrillo MC. 2007. Involvement of reactive oxygen species on the apoptotic mechanism induced by IFN-α2b in rat preneoplastic liver. Biochemical Pharmacology 73:1776–1785.

53. Fink K, Martin L, Mukawera E, Chartier S, De Deken X, Brochiero E, Miot F, Grandvaux N. 2013. IFNβ/TNFα synergism induces a non-canonical STAT2/IRF9-dependent pathway triggering a novel DUOX2 NADPH Oxidase-mediated airway antiviral response. Cell Res 23:673–690.

509 54. Dobin A, Davis CA, Schlesinger F, Drenkow J, Zaleski C, Jha S, Batut P, Chaisson M, Gingeras TR. 2013.
510 STAR: ultrafast universal RNA-seq aligner. Bioinformatics 29:15–21.

511 55. Love MI, Huber W, Anders S. 2014. Moderated estimation of fold change and dispersion for RNA-seq data
512 with DESeq2. Genome Biol 15.

513

514

FIGURE LEGENDS

Figure 1. Increased WNV Replication in TRIM6-KO Cells is Associated with Impaired IFN-I Induction and Signaling. Growth kinetics for WNV 385-99 (MoI 0.1) in wildtype (wt) and TRIM6-KO A549 cells. Viral load in cell culture supernatants of infected cells was determined by plaque assay on Vero CCL-81 cells (A). Expression levels of total and phosphorylated proteins in whole cell lysates from WNV 385-99 infected cells (MoI 0.1) were analyzed by western blot (B). mRNA expression profile of *Ifnb*, or ISGs: *Isg54*, *Oas1*, *Irf7 and Stat1*, and or inflammatory *Il6* genes from WNV 385-99 infected cells (MoI 5.0) (C). Change in expression represented as fold induction over mock infected cells, and normalized by 18s (C). Error bars represent standard deviation. For statistical analysis, two-way ANOVA with Bonferroni's post-test for multiple comparisons (A and C) was used; ****p <0.0001, ***p <0.001, **p <0.01, *p <0.05. All experiments were performed in triplicate and repeated three times.

Figure 2. IFN-I Pre-treatment is Less Efficiently Antagonizes WNV Replication in TRIM6-KO Cells. wt or TRIM6-KO cells were treated with recombinant human IFNβ-1a (100U) for 4 hours prior to infection with WNV 385-99 (MoI 5.0) for 24 hours. Supernatants from infected cells were titrated and viral load was calculated via plaque assay. Error bars represent standard deviation. One-way ANOVA with Tukey's post-test was performed to assess statistical significance; ****p <0.0001, *p <0.05. Fold change reported in parenthesis. All experiments were performed in triplicate.

Figure 3. Transcription of Canonical Interferon-Stimulated Genes and VAMP8 are Down-Regulated in TRIM6 Knockout Cells. Transcriptional profiling of cellular mRNA by Next Generation Sequencing of mock (A) or WNV 385-99 infected (MoI 5.0) (B) wt or TRIM6 KO A549 at 24 hours post-infection. Log_2 fold change was calculated as TRIM6-KO/mock with genes down-regulated in

TRIM6-KO cells on the left (negative values) and up-regulated in TRIM6-KO cells on the right (positive values). The $-\log_{10}$ p-value represents the significance. VAMP8 data point is represented as a light grey square and interferon-simulated genes (ISGs) are represented as dark grey triangles. ISGs in A: *Oasl* and *Trim31* and B: *Hla-dma*, *Hla-dmb, Ifi27*, *Ifitm1*, *Ifitm2*, *Ifitm3*, *Ifi30*, *Ifi35*, *Ifi44l*, *Mx2*, *Oas2*, *Trim14*, *Pml/Trim19*, *Trim31*, *Trim34*, *Zbp1*. Validation of VAMP8 expression at the protein (C) or RNA (D) levels in wt or TRIM6 KO cells. Error bars represent standard deviation and VAMP8 expression validation experiments were performed in triplicate and repeated three times.

Figure 4. Depletion of VAMP8 Impairs STAT1 Activation during WNV Infection but does not alter WNV Replication. WNV 385-99 (MoI 0.1) growth kinetics in wt A549 cells treated with non-targeting control (control) or VAMP8-targeting (VAMP8) siRNAs for 24 hours prior to infection. Viral load in cell culture supernatants of infected cells was determined by plaque assay on Vero CCL-81 cells (A). Expression levels of total and phosphorylated proteins in whole cell lysates from WNV 385-99 infected cells (MoI 0.1) were analyzed by western blot (B). Error bars represent standard deviation. A two-way ANOVA with Bonferroni's post-test was applied to assess differences in viral load (A), but there were not significant differences between control and VAMP8 siRNA treated cells. Experiment performed in triplicate and repeated three times.

Figure 5. VAMP8 Knockdown Inhibits IFN-I Signaling following IFNβ Treatment. Translational expression levels of total and phosphorylated STAT1 in wt A549 cells following treatment with non-targeting control (siControl) or VAMP8-targeting (siVAMP8) siRNAs for 24 hours followed by treatment with recombinant human IFNβ-1a (500U/mL) for 12 hours (A). Transcriptional expression levels of *Isg54*, *Oas1*, and *Stat1* genes analyzed by qRT-PCR. Data were normalized to 18s (B). Gene expression data were analyzed using one-way ANOVA with Tukey's post-test to assess

563 statistical significance; p**** <0.0001, p*** <0.001, p* <0.05. Experiments performed in triplicate and
564 repeated three times.
565
566 **Figure 6. WNV Replication is Enhanced in VAMP8 Knockdown Cells Following Pre-treatment**
567 **with IFNβ.** wt A549 cells were treated with non-targeting control (control) or VAMP8-targeting
568 (VAMP8) siRNAs for 24 hours then treated with recombinant human IFNβ-1a for 16 hours prior to
569 infection with WNV 385-99 (MoI 5.0) for 24 hours. Supernatants from infected cells were titrated and
570 viral load was calculated via plaque assay. Error bars represent standard deviation. One-way ANOVA
571 with Tukey's post-test was performed to assess statistical significance; ****p <0.0001, *p <0.05. Fold
572 change reported in parenthesis. Experiment completed in triplicate.
573
574 **Figure 7. Graphical Summary.**
575 Following virus infection, viral RNA is recognized by pathogen recognition receptors (PRRs). PRRs
576 then signal through their adaptors, triggering the activation of kinases TBK1 and IKKε, which
577 phosphorylate and activate the transcription factor IRF3. Once activated, IRF3 translocates to the
578 nucleus and, in concert with other factors not indicated, promotes the transcription of IFNβ. IFNβ is
579 then secreted and signals in an autocrine or paracrine manner through the type I IFN receptor
580 (IFNAR). The kinases (Jak1 and Tyk2) associated with IFNAR then facilitate the phosphorylation of
581 STAT1 at tyrosine (Y) 701 and STAT2 in an IKKε-independent manner. Phosphorylated STAT1 and
582 STAT2 interact with IRF9 to form the ISGF3 complex, which translocates to the nucleus to promote
583 the transcription of genes with interferon stimulated response elements (ISRE) including *Stat1, Oas1,*
584 and *Isg54*. In addition to IKKε independent IFN-I signaling, the E3 ubiquitin ligase TRIM6 facilitates
585 IKKε-dependent IFN-I signaling. TRIM6, in coordination with the ubiquitin activating (UbE1) and
586 ligating (UbE2K) enzymes to facilitate the formation of K48-linked unanchored poly-ubiquitin chains,

which act as a scaffold for the oligomerization and cross-phosphorylation of IKKε at threonine (T) 501(30). TRIM6 also facilitates activation of IKKε during IFN-I induction. During IFN-I signaling, activated IKKε phosphorylates STAT1 at serine (S) 708. STAT1 phosphorylation at S708, an IKKε-dependent modification, facilitates the formation of an ISGF3 complex with different biophysiological properties which allows the ISGF3 complex to have enhanced binding to certain ISRE-containing promoters ultimately inducing a different ISG profile than when STAT1 is phosphorylated at Y701 (29, 40). Although the mechanism is currently unknown (question mark), TRIM6 induces VAMP8 expression, which in turn is important for inducing optimal IFN-I signaling modulating STAT1 phosphorylation at Y701, and an efficient antiviral response.

Table S1. qRT-PCR primers

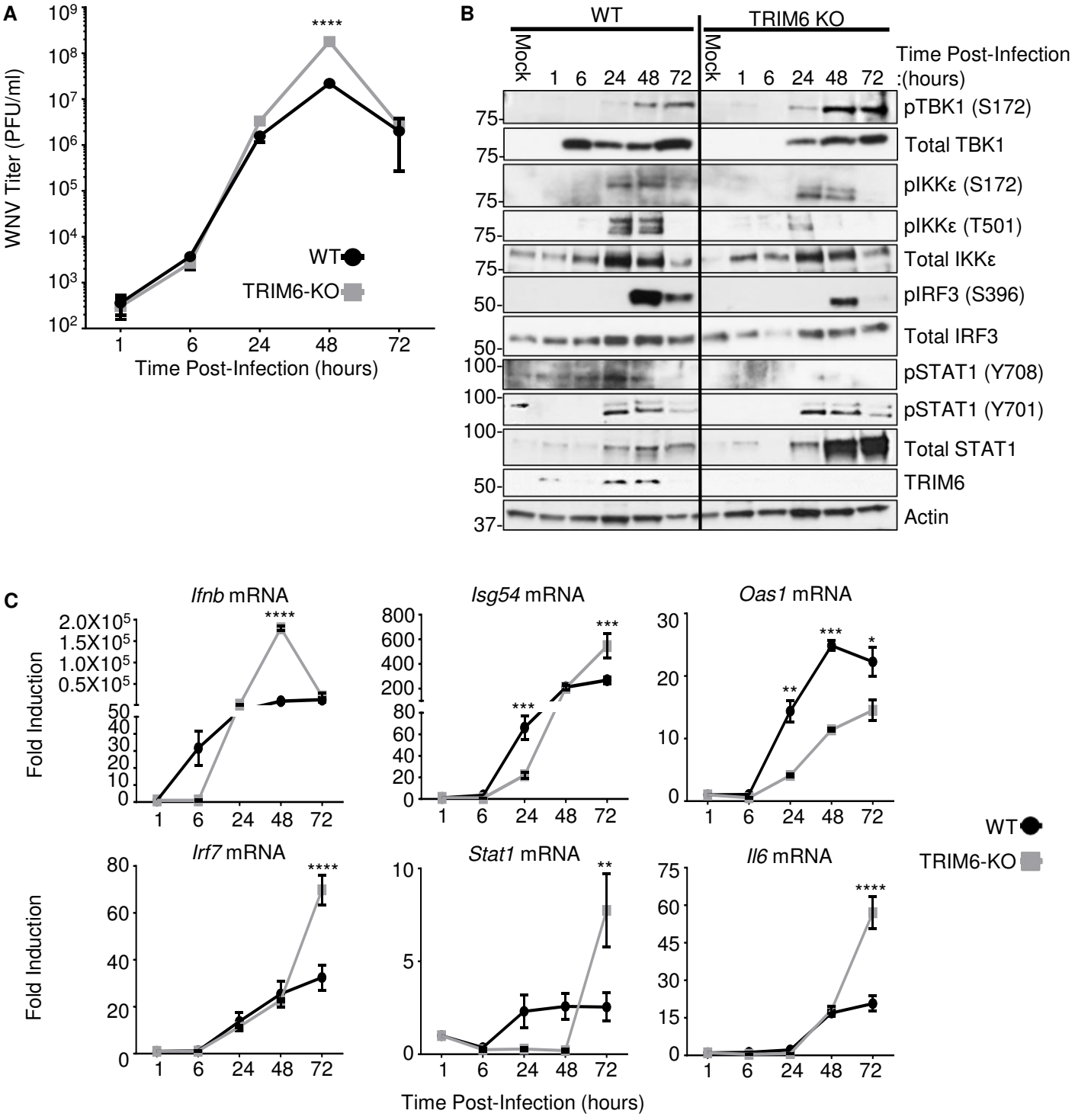

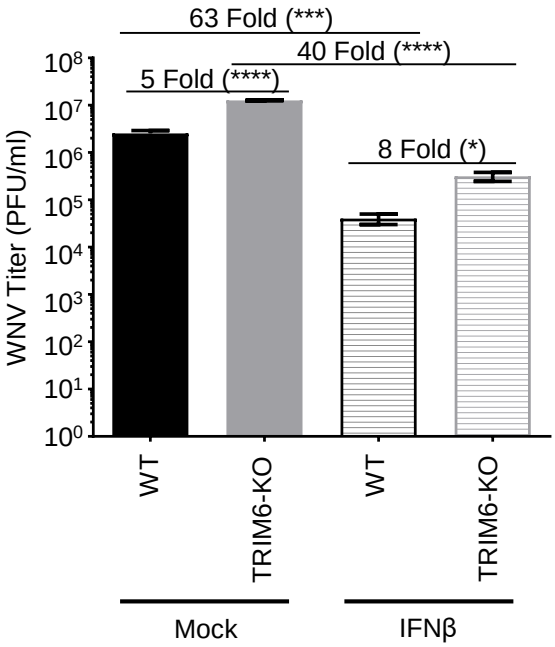

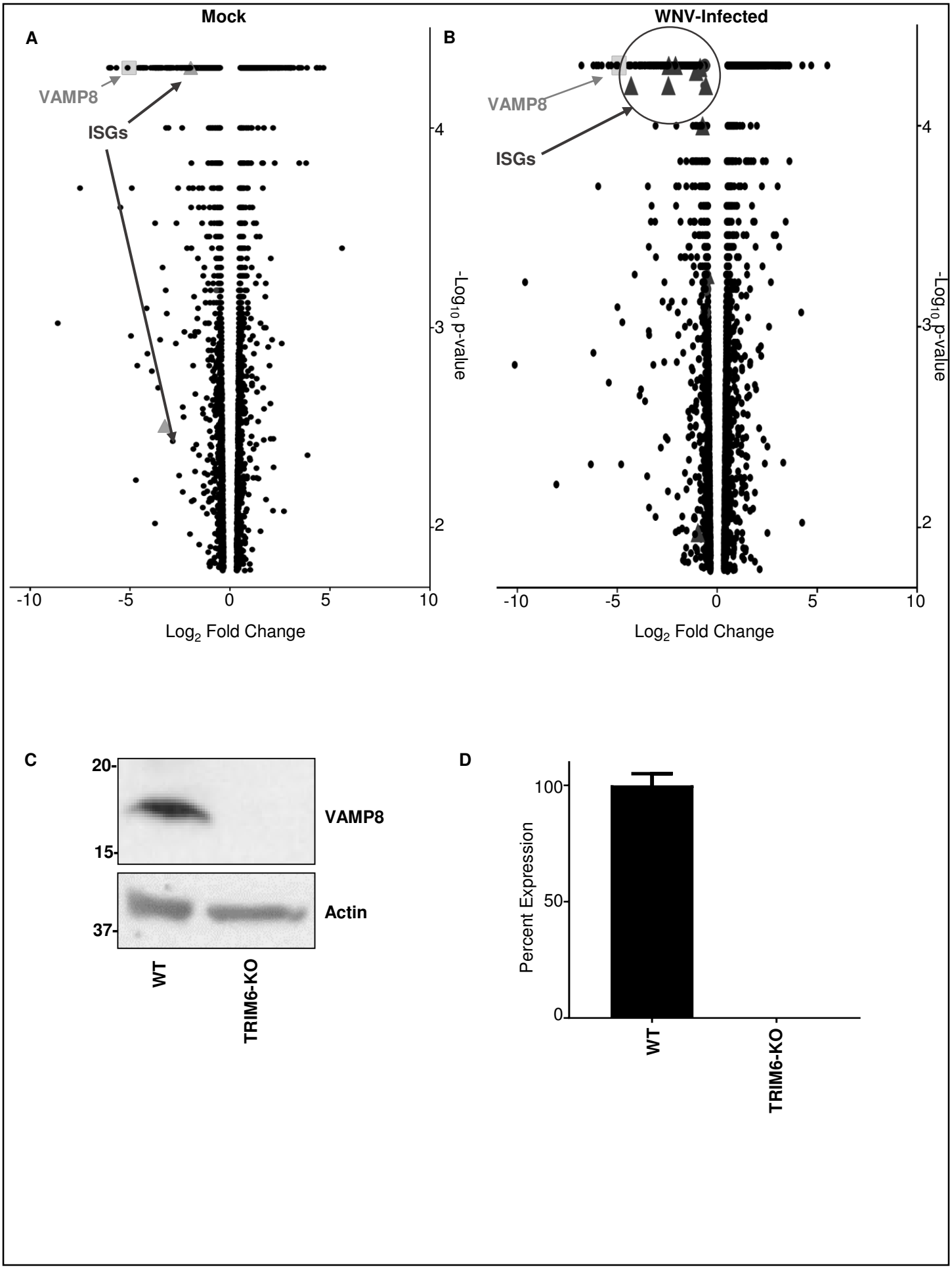

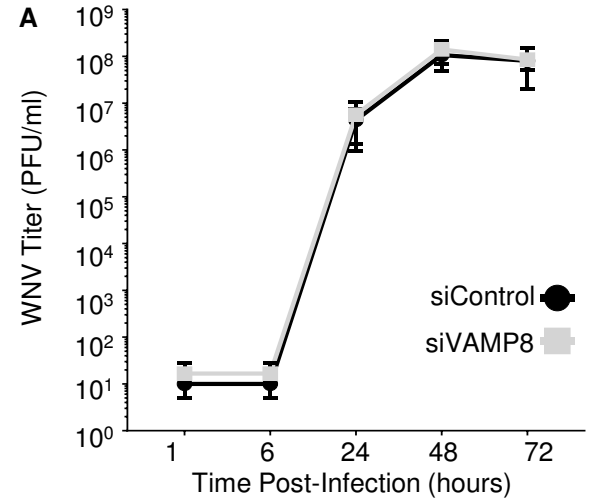

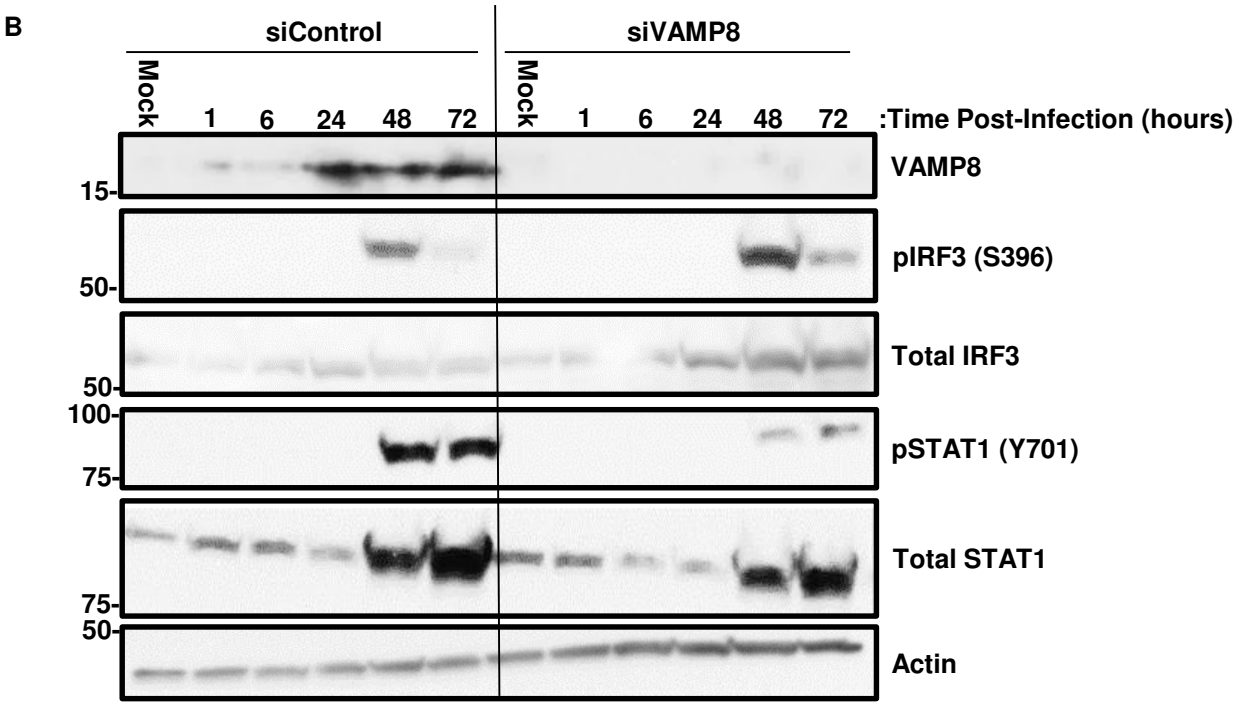

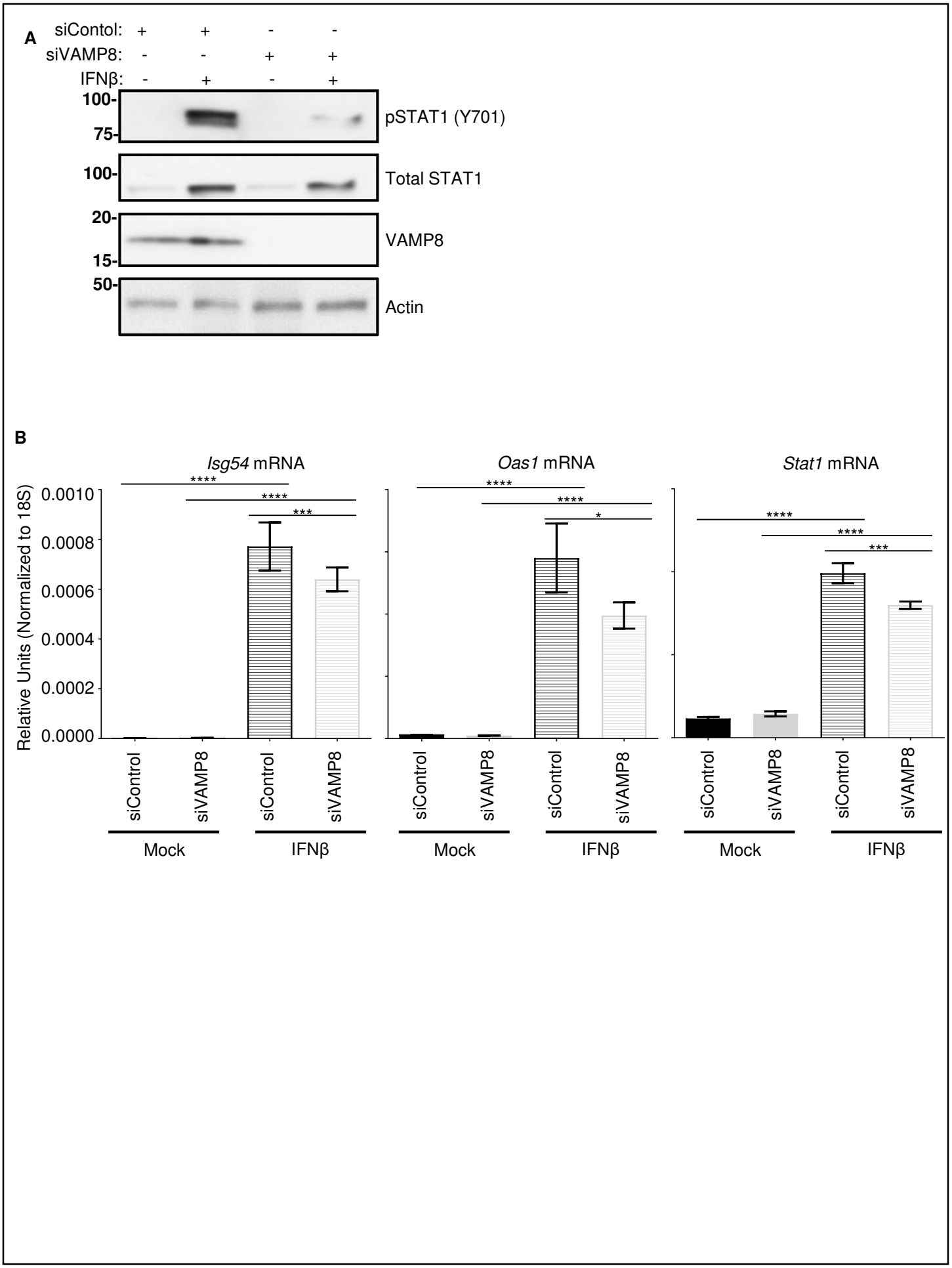

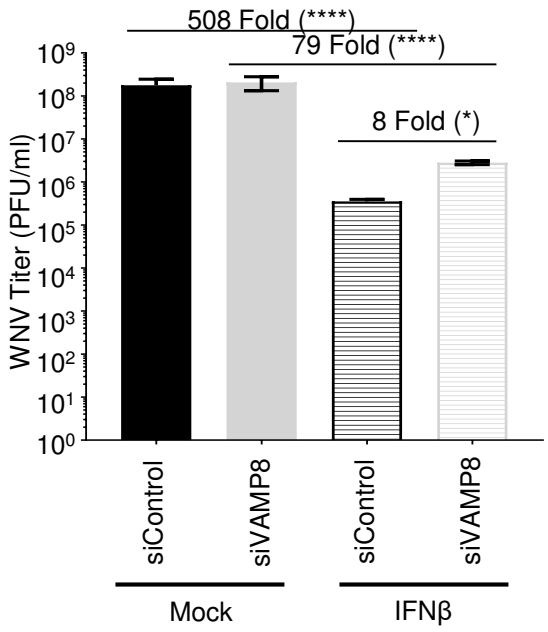

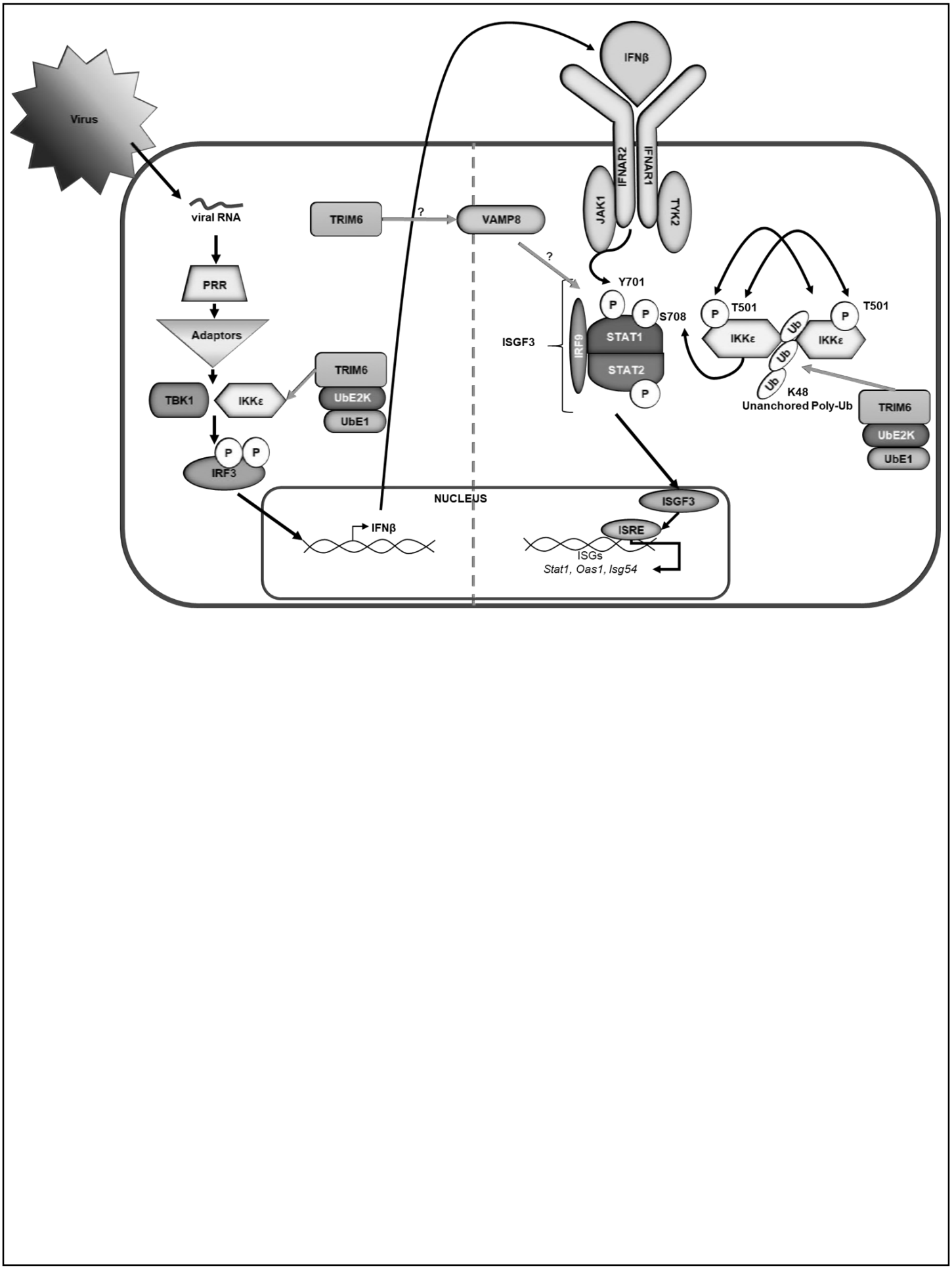

Primer Name	Primer Sequence
18S F	GTAACCCGTTGAACCCCATT
18S R	CCATCCAATCGGTAGTAGCG
Ifnb F	TCTGGCACAACAGGTAGTAGGC
Ifnb R	GAGAAGCACAACAGGAGAGCAA
Il6 F	AGAGGCACTGGCAGAAAACAAC
Il6 R	AGGCAAGTCTCCTCATTGAATCC
Irf7 F	CGCGGCACTAACGACAGGCGAG
Irf7 R	GCTGCCGTGCCCGGAATTCCAC
Isg54 F	ATGTGCAACCCTACTGGCCTAT
Isg54 R	TGAGAGTCGGCCCAGTGATA
Oas1 F	GATCTCAGAAATACCCCAGCCA
Oas1 R	AGCTACCTCGGAAGCAGGTT
Stat1 F	ACAGCAGAGCGCCTGTATTG
Stat1 R	CAGCTGATCCAAGCAAGCAT
Vamp8 F	CTTGGAACATCTCCGCAACA
Vamp 8 R	CGCTGAACACAGAACTTGAG